



**HAL**  
open science

# Nanofluids dynamic viscosity evolution using high-frequency acoustic waves: application applied for droplet evaporation

Ibrahim Zaaroura, Malika Toubal, Julien Carlier, Souad Harmand, Bertrand Nongaillard

► **To cite this version:**

Ibrahim Zaaroura, Malika Toubal, Julien Carlier, Souad Harmand, Bertrand Nongaillard. Nanofluids dynamic viscosity evolution using high-frequency acoustic waves: application applied for droplet evaporation. *Journal of Molecular Liquids*, 2021, 341, pp.117385. 10.1016/j.molliq.2021.117385 . hal-03364913

**HAL Id: hal-03364913**

**<https://hal.science/hal-03364913>**

Submitted on 25 May 2023

**HAL** is a multi-disciplinary open access archive for the deposit and dissemination of scientific research documents, whether they are published or not. The documents may come from teaching and research institutions in France or abroad, or from public or private research centers.

L'archive ouverte pluridisciplinaire **HAL**, est destinée au dépôt et à la diffusion de documents scientifiques de niveau recherche, publiés ou non, émanant des établissements d'enseignement et de recherche français ou étrangers, des laboratoires publics ou privés.

1  
2  
3  
4  
5  
6  
7  
8  
9  
10  
11  
12  
13  
14  
15  
16

**Nanofluids dynamic viscosity evolution using high-frequency acoustic waves:  
Application applied for droplet evaporation**

Ibrahim Zaaroura <sup>a,b</sup>, Malika Toubal <sup>b</sup>, Julien Carlier <sup>b</sup>, Souad Harmand <sup>a</sup>, Bertrand Nongaillard <sup>b</sup>

a- Univ. Polytechnique Hauts-de-France, CNRS, UMR 8201- LAMIH - Laboratoire d'Automatique de Mécanique et d'Informatique Industrielles et Humaines, F-59313 Valenciennes, France

b- Univ. Polytechnique Hauts-de-France, CNRS, Univ. Lille, YNCREA, Centrale Lille, UMR 8520 - IEMN -DOAE, F-59313 Valenciennes, France

1  
2  
3  
4  
5  
6  
7  
8  
9  
10  
11  
12  
13  
14  
15  
16  
17  
18  
19  
20  
21  
22  
23  
24  
25  
26  
27  
28  
29

**Abstract**

Many interests are shown on nanofluids as it's suitable for cooling applications. Knowing the physical properties of nanofluids such as viscosity plays a key role in practical heat transfer situations. The main goal of this work is to measure the dynamic viscosity of Gold nanofluids during sessile droplets evaporation, at ambient temperature, based on ultrasonic high-frequency acoustic waves (1 GHz). So, we have developed the high-frequency acoustic transducers, for longitudinal and shear waves, located at the bottom side of the silicon substrate. This method has access to characterize the liquid/solid interface (Droplet/Silicon). Due to viscoelastic losses (one of the causes of attenuation), the attenuation (attenuation in fluids about 220 dB/mm) of the sound energy produced by nanofluid generates a complex form for the mechanical impedance of the sessile droplet of nanofluid. The measured echoes diagram represented by amplitude and phase angle were obtained using a Network Analyzer. The complexity of the nanofluid for the shear signal wave has a direct relation between the attenuation and the viscosity and as a result, an online variation in the shear viscosity of a droplet contains 4% C<sub>v</sub> gold nanoparticles were extracted throughout the evaporation process. At the same time, a new micromechanical model developed by FreeFem++ software was provided to compare the results obtained experimentally. This model has been validated to be used to calculate the viscosity of nanofluids.

**Keywords:** Nanofluids; Droplets Evaporation; Acoustic field; Shear viscosity; Finite element Model

## 1 List of Symbols

2

$C_v$	Volume concentration, %
$r^*$	Complex reflection coefficient
$ R $	Amplitude reflection coefficient
$R_{LL}$	Longitudinal reflection coefficient
$R_{TT}$	Shear reflection coefficient
$Z_{si}$	Mechanical Impedance of silicon substrate, $\text{kg}\cdot\text{s}^{-1}\cdot\text{m}^{-2}$
$Z_{nf}$	Mechanical Impedance of droplet nanofluid, $\text{kg}\cdot\text{s}^{-1}\cdot\text{m}^{-2}$
$C$	Acoustic velocity, $\text{m}\cdot\text{s}^{-1}$
$C_L$	Longitudinal acoustic velocity, $\text{m}\cdot\text{s}^{-1}$
$C_T$	Shear acoustic velocity, $\text{m}\cdot\text{s}^{-1}$
$nf$	Nanofluid
$p$	Particles
$w$	Water
$\rho_{nf}$	Density of Nanofluid, $\text{kg}\cdot\text{m}^{-3}$
$\rho_p$	Density of nanoparticles, $\text{kg}\cdot\text{m}^{-3}$
$\rho_w$	Density of water, $\text{kg}\cdot\text{m}^{-3}$
$E_{nf}$	Young Modulus of nanofluid, Gpa
$E_w$	Young Modulus of Water, Gpa
$E_p$	Young Modulus of nanoparticle, Gpa
$\emptyset$	Phase angle, °
$\omega$	Pulsation of the incident wave
$C_T$	Shear acoustic velocity, $\text{m}\cdot\text{s}^{-1}$
$\alpha_T$	Shear attenuation
$k_T^*$	Complex shear wave number, $\text{m}^{-1}$
$\mu_s$	Shear viscosity, Pa.s
$v_p$	Particle Volume Fraction
$\sigma_{12}^0$	Shear stress, $\text{N}\cdot\text{m}^{-2}$
$\mu$	Lame coefficient, Gpa
$\varepsilon$	Deformation, SI

3

4

1

## 2 **I-Introduction**

3 Nanofluids as a new innovative class of heat transfer fluids represent a rapidly emerging field  
4 where nanoscale science and thermal engineering meet [1, 2]. It's a novel strategy to improve  
5 heat transfer characteristics of fluids by the addition of solid particles with diameters below  
6 100 nm due to their high thermal performance compared to their base fluids (Solid metal has a  
7 larger thermal conductivity than a base fluid). This basic idea of particle-dispersed fluid can be  
8 traced back to Maxwell's study in 1873 [3]. Since nanofluids exhibit unprecedented heat transfer  
9 properties [4, 5], it considered as potential working fluids to be used in high heat flux systems  
10 such as electronic cooling systems, solar collectors, heat pipes, heating building and nuclear  
11 reactors. [6-8]

12 To clarify our research on nanofluids in improving heat transfer in thermal engineering systems  
13 and before design any thermal system in which nanofluid is the working fluid, it is necessary to  
14 know their thermo physical properties including thermal conductivity [9], viscosity [10], density  
15 and heat capacity in addition to the stability of nanoparticles inside the fluids [11, 12]. Few  
16 studies have been conducted on the rheology of nanofluids [13-15], even though the viscosity of  
17 nanofluid is as important as thermal conductivity when it comes to practical applications.  
18 Measuring the viscosity of the nanofluids is very important since it indicates the fluid's  
19 resistance.

20 Several research presented the viscosity effect on the evaporation rate of droplets with  
21 nanoparticles compared to their base fluids [16, 17]. Many parameters affect the nanofluid  
22 viscosity including preparation method, base fluid type, temperature, particle aggregation,  
23 particle size and shape, volume concentration , surfactants, and so on [18, 19]. As a result, the  
24 efficiency of heat transfer performance is reduced even if it shows a high thermal conductivity.  
25 Different methods were used to measure the viscosity of nanofluids using mechanical method  
26 (rheological), Rheometer (rotational, capillary...) [20-22]. Measuring the properties of a material  
27 using rheological method which contains the drive motor and encoder which measure and set the  
28 torque, deflection angle and speed then we can calculate the viscosity needed.

29 In addition to some theoretical models presented in the literature to estimate the shear viscosity  
30 of nanofluids such as Brinkman model [23], Einstein model [24], Brownian model [25]. Most of  
31 these models give only a good accuracy at lower volume concentration percentage compared to

1 the mechanical experimental results while at higher percentage the theorem showed less  
2 accuracy [26-28].

3 Experimental investigation is very important for the analysis and validation of theoretical  
4 models proposed by researchers. Thus, in this work, we have introduced a high frequency  
5 ultrasonic technique to measure the viscosity of nanofluids during droplets evaporation.  
6 Ultrasound has found a wide range of applications in the measurement of the viscosity of liquids  
7 [29, 30]. In this experiment, we measured locally the effective shear viscosity, as a continuous  
8 measurement, of a sessile droplet contains gold nanoparticles (Au-water) during evaporation  
9 process. This method based on acoustical point of view at the solid-liquid interface. Our  
10 acoustical measurements were done at very high frequency (1 GHz) in order to give us a very  
11 good sensitivity at the interface (Silicon- droplet). Few works have been done to find the  
12 viscosity using acoustics methods but all deal only at low frequency and for pure liquids only  
13 (frequency doesn't not exceed 100 MHz) which is less sensible [31-33].

14 The acoustic method, developed in our laboratory, was used to characterize solid-liquid  
15 interfaces at micro/nanometer scales [34] [16]. Experiments on the evaporation of nanofluid  
16 sessile droplets at ambient temperature are conducted to measure the shear viscosity of gold  
17 nanofluid droplet during evaporation process. The analysis was depended on the reflection  
18 coefficient from the wave signal that emitted at the bottom of the silicon substrate and reach this  
19 signal to the bottom of the droplet using a two transducer one refers to the measurement droplet  
20 while the other to the reference air. At this high frequency signals, the characteristic of  
21 nanoparticles deposited at the surface are clearly observed with the change in the reflection  
22 amplitude [12]. In this case, we estimate the attenuation (viscoelastic loses) only in the liquid and  
23 then the reflection coefficient will have a complex form (amplitude and phase angle) for each  
24 longitudinal and shear waves. This complexity related to the mechanical impedance of both the  
25 substrate and the nanofluid droplet deposited at the interface.

26 Measuring the acoustical properties such as velocity, attenuation, and phase changes resulting  
27 from wave reflections are often used as a tool for rheological characterization of liquid  
28 (solid/liquid interface). From the shear reflection waves, the shear viscosity of the gold nanofluid  
29 sessile drop is obtained throughout the evaporation process. Also, an estimate of the particle  
30 concentrations, at the interface, throughout the process was deduced from the longitudinal  
31 waves. At the same time, we presented in this work our micromechanical model developed in  
32 FreeFem++ to calculate the effective shear viscosity of nanofluids depending on their

1 nanoparticles concentration. The concept is to find the creep function under a constant applied  
 2 stress on 2D Kelvin Vogt medium (fluids with particles) and from the theoretical expression we  
 3 extract the needed parameters. This model was validated and approved in [35] for nanofluids  
 4 viscosity measurements.

## 5 **II- Material and Methods**

### 6 **1- Viscosity measurements using high frequency acoustic waves (1 GHz)**

7  
 8 The study is dependent on the mechanical properties at the interface between the silicon substrate  
 9 and the droplet. It is represented by a reflection coefficient. The formula in **Eq. (1)** has a complex  
 10 form and it is related to the mechanical impedance of the substrate and the liquid where it is  
 11 deposited at the interface. The complexity is due to viscoelastic losses inside the sessile droplet  
 12 (Attenuation).

$$13 \quad r^* = \frac{Z_{nf}^* - Z_{si}}{Z_{si} + Z_{nf}^*} \quad (1)$$

14 Where  $Z = \rho.C$ ,  $\rho$  is the density of the medium, and  $C$  is the acoustic velocity of the wave  
 15 propagating inside of the medium. In our case,  $Z_{si}$  is the acoustic impedance of the (100) silicon  
 16 (Crystalline orientation of the silicon crystal) substrate and  $Z_{nf}^*$  is the complex acoustic  
 17 impedance taking into account the attenuation in the nanofluid droplet. The reflection coefficient  
 18 can be written in the complex form as follow:

$$r^* = |R| \exp(i\phi) \quad (2)$$

19 Where  $|R|$  is the amplitude of the reflection coefficient,  $\phi$  the phase angle between the incident  
 20 and reflected wave. We present in **Table 1**, the longitudinal, shear speed of sound and the  
 21 density of silicon to identify subsequently the acoustic impedances in each case.

Medium	Longitudinal Acoustic Velocity, $C_L$ (m/s)	Shear Acoustic Velocity, $C_T$ (m/s)	Density, $\rho$ (kg.m <sup>-3</sup> )
Silicon	8434	5843	2300
Water	1488	88	998

22

**Table 1.** Physical properties of silicon and water at room temperature. [36]

The reflection coefficients are determined for both longitudinal reflected waves and shear reflected waves during droplet evaporation process. The shear viscosity measurement will be obtained from the amplitude and the phase angle of the shear waves.

The expression of the complex shear reflection coefficient  $r_{TT}^*$  is given in **Eq. (3)**. The complex shear wave number  $k_T^*$  is correlated to  $r_{TT}^*$  as in **Eq. (4)**.

$$r_{TT}^* = \frac{Z_{nf}^* - Z_{si}}{Z_{si} + Z_{nf}^*} = \frac{\rho_{nf} C_T^* - Z_{si}}{Z_{si} + \rho_{nf} C_T^*} = |R| \exp(i\phi) = A + iB \quad (3)$$

$$C_T^* = \omega / k_T^*$$

Where  $\rho_{nf}$  is the density of nanofluid,  $C_T^*$  is the complex shear velocity in nanofluid,  $\omega$  the frequency of the incident wave and  $k_T^*$  the complex shear wave number. From these equations, we can know the complex shear wave number in function of shear reflection coefficient.

$$k_T^* = \frac{k_{si} \rho_{nf} (1 - r_{TT}^*)}{\rho_{si} (1 + r_{TT}^*)} = a - jb \quad (4)$$

Where  $k_T^*$  can be express as follow:

$$k_T^* = \omega / C_T - i\alpha_T = \omega / C_T - i \sqrt{\frac{\rho_{nf} \omega}{2\mu_s}} \quad (5)$$

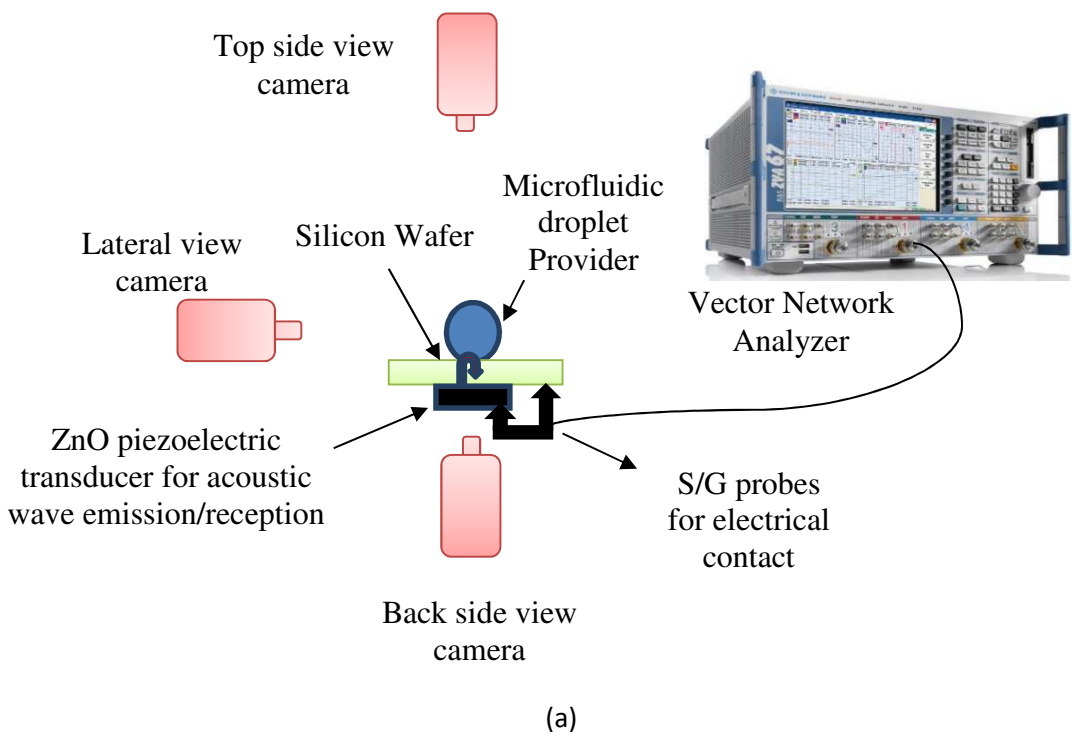
Where  $C_T$  the effective shear velocity in nanofluid and  $\alpha_T$  is the shear attenuation and  $\mu_s$  is the shear viscosity. One can see that from the kinetics of both the amplitude and the phase angle of the shear wave, the shear viscosity can be deduced at the interface between the substrate and the nanofluids droplet during its evaporation process.

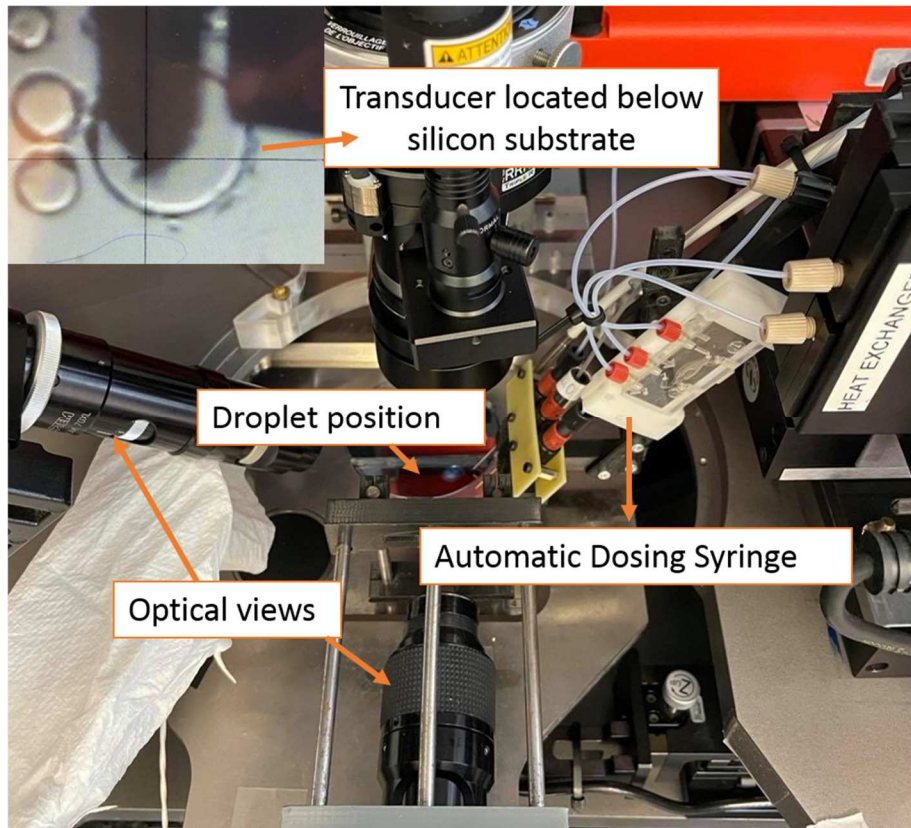
## 2- Experimental setup

In this work, the studied nanofluid consists of gold (Au) nanoparticles (Sigma Aldrich, 5 nm diameter, OD 1, stabilized suspension in 0.1 mM PBS, reactant free with volume concentration of 4% C<sub>v</sub>) dissolved in distilled water and then stabilized through ultra-sonication (Elma, S 10/H) for at least 1 h before use.



1 The experimental set up is similar to the one used in a previous study [Zaaroura et al., 2018] [12].  
 2 Measurements are made on a high frequency echography principle and under a controlled  
 3 atmosphere using an air-conditioning system. A cascade PM8 prober system is used to control  
 4 the position S/G (signal/ground) probe at the micro scale level on a piezoelectric transducer as a  
 5 small as 250  $\mu\text{m}$  in diameter to achieve electrical measurements (see **Fig. 1**).  
 6 The specificity of the probe is the possibility to achieve an electrical contact at the backside of  
 7 the wafer on which the piezoelectric transducer was fabricated [Annex A]. These probes are  
 8 connected to a Rhode & Schwarz ZVA8 Vector Network Analyzer. A Rohde & Schwarz ZVA8  
 9 Vector Network Analyzer allows the measurement of the reflection coefficient in the time  
 10 domain such as the phase angle between the incident wave and those reflected.





(b)

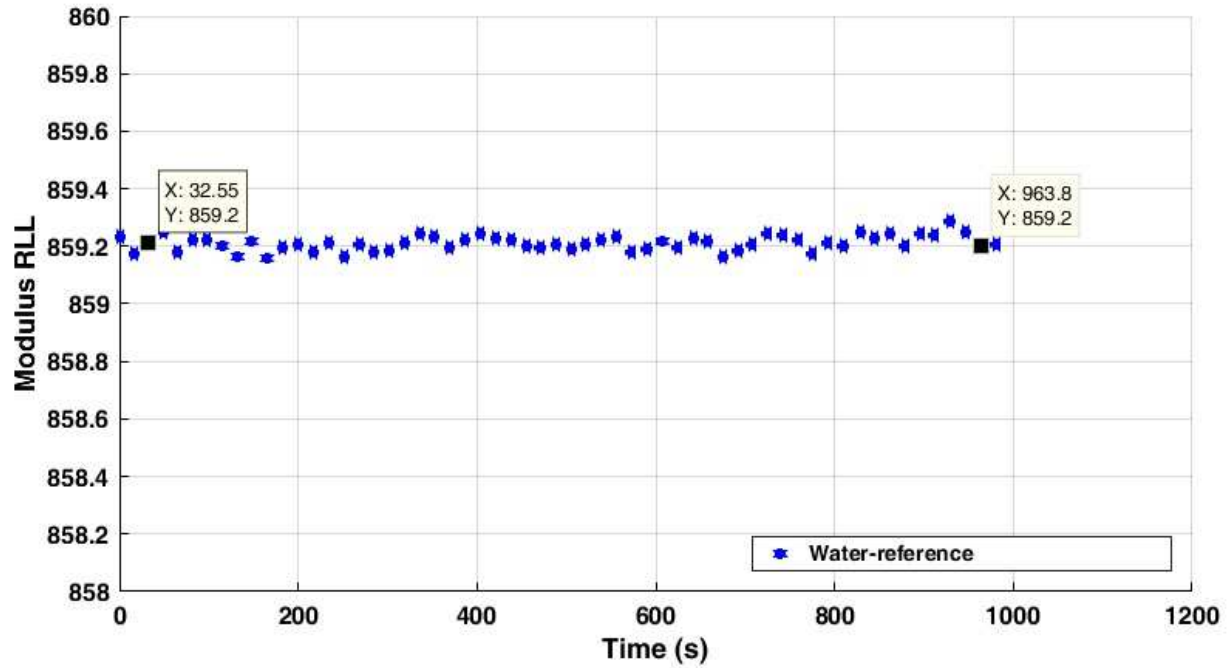
**Figure 1.** (a) Schema of the experimental setup of acoustic measurements, (b) Experimental setup in real state.

To ensure and verify the accuracy of our acoustic method, the used transducer was fabricated with specific technique in order to generate more shear waves since it is the most sensitive parameter to extract the shear viscosity. This method known as a blind technique, see [Annex A].

### III- Results and Discussion

#### 1- A calibration method for acoustic measurements: Water as a reference liquid

Several precautions are taken into consideration to improve measurements accuracy. A 2  $\mu\text{l}$  drop of water, as reference liquid, is deposited on the hydrophobic silicon surface where the transducer (250  $\mu\text{m}$  in diameter) is located. An acoustic wave is generated by the ZnO transducer through the substrate to the interface. Then, the evolution in the amplitude reflection coefficient is determined and represented in Fig. 2.



1

2 **Figure. 2.** Amplitude reflection coefficient evolution of pure water droplet during evaporation  
 3 process at 22°C.

4 The amplitude coefficient is determined to be 0.8593 theoretically since we know all the physical  
 5 properties of water.

6 The experimental result, as shown in **Fig. 2**, demonstrates a good reliability of the measured  
 7 amplitude coefficient  $|R| = 0.8592 \pm 0.01\%$ . At the same, the shear phase angle of water is also  
 8 extracted and represented in **Fig. 4** for viscosity measurements.

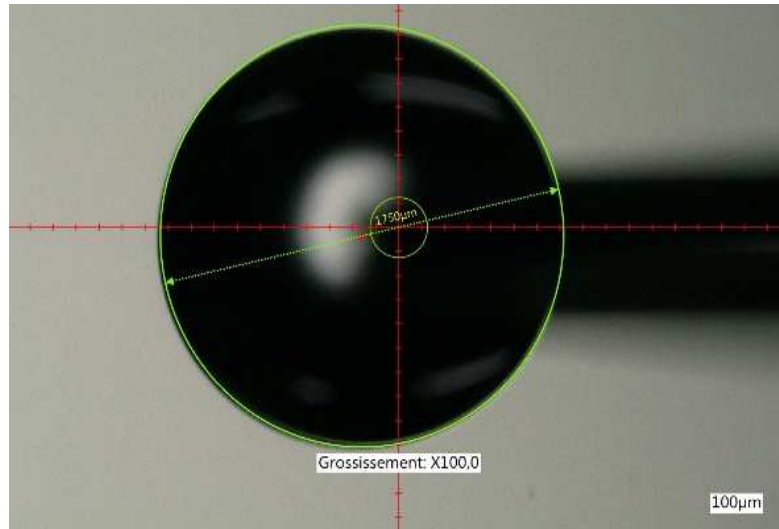
9

10 **2- Measurements of the viscosity of (4% C<sub>v</sub>) Gold nanofluids droplet**

11

12 The measurements were carried out during a droplet of gold nanofluid (4% C<sub>v</sub> - 2μl drop) at  
 13 ambient temperature, 22° C. The variation in the amplitude (R<sub>LL</sub>) and phase angle (R<sub>TT</sub>) of the  
 14 reflected waves, sent to the interface, were found throughout the evaporation process, **Fig. 3** and

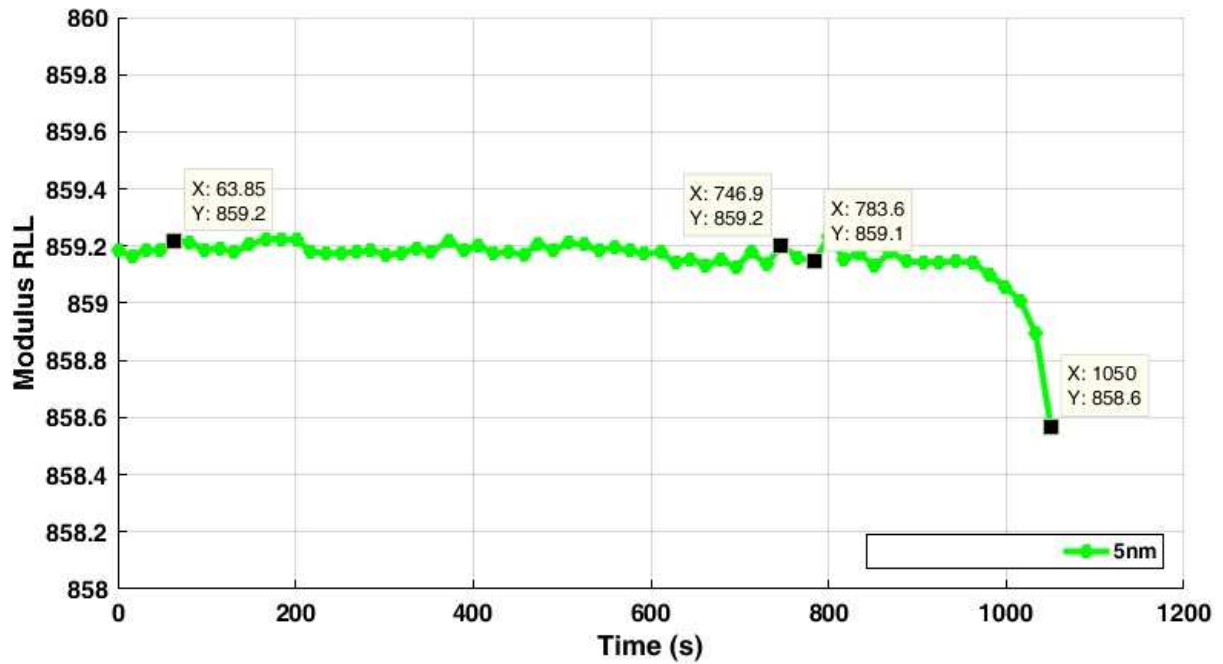
15 **Fig. 4.**



1

2

(a)



3

4

(b)

5 **Figure. 3.** (a) 4 %  $C_v$  Gold nanofluid droplet deposited on silicon substrate and above the  
 6 transducer of 250 $\mu\text{m}$  in diameter (b) Amplitude reflection coefficient ( $R_{LL}$ ) evolution of 4%  $C_v$   
 7 Au-water nanofluid droplet evaporation on a silicon substrate at 22°.

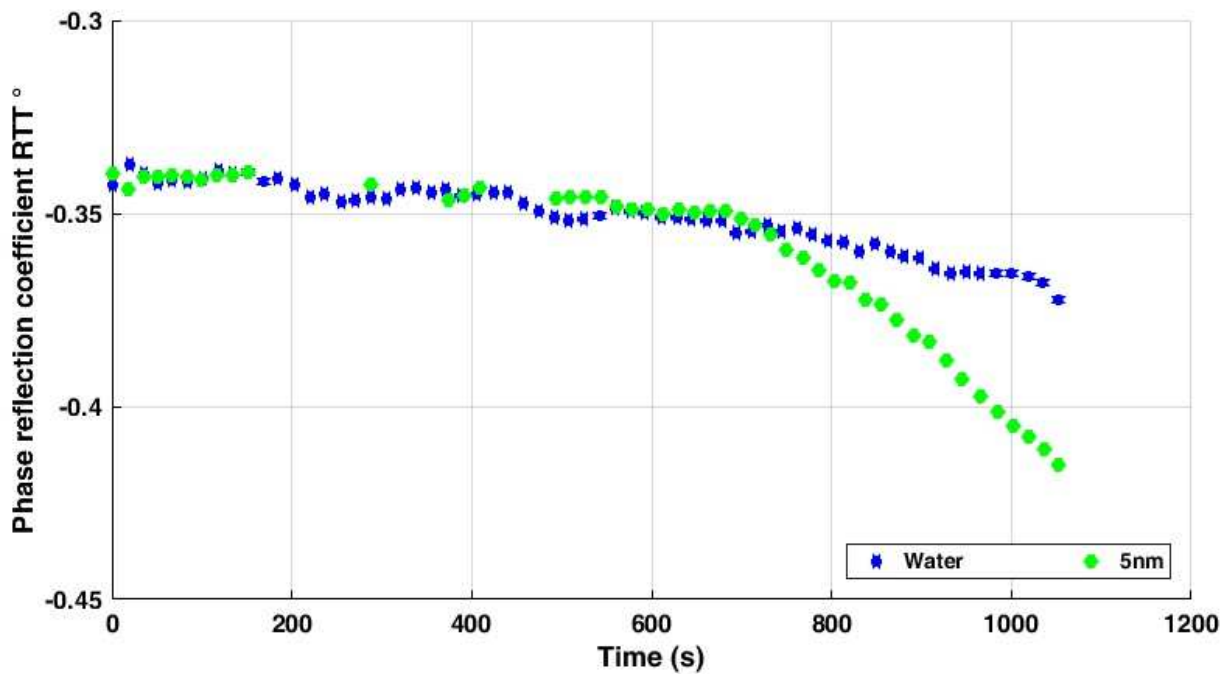
8

9 We can observe from **Fig. 3** that the amplitude reflection coefficient was remained constant  
 10 during about 800 s then begins to change and decreasing till the end of evaporation process. This  
 11 is primarily ascribed to a change of the physical properties of the material interacting with the  
 12 ultrasounds at the interface. This evolution (after 800 s) is clearly due to the precipitation of gold

1 (Au) nanoparticles on the silicon substrate above the transducer. The delay in the gold particles  
2 deposition due to the good stability of these particles after suspension in 0.1 mM PBS [16].

3 In **Fig. 4**, we represent the shear phase angle variation for both water and gold nanofluid during  
4 droplet evaporation process. These evolutions are more representative and sensitive than the  
5 amplitude of reflection coefficient for viscosity measurements. So, after 800 s, the phase angle  
6 rapidly **decreases** as a function of time. This sensitivity will entails higher variation in the  
7 viscosity after from  $t=800$  s till the end of the evaporation process. From these results and  
8 according to **Eqs. 3, 4 and 5** we can obtain the variation in shear viscosity of gold nanofluid  
9 droplet during evaporation process. (See **Fig. 5**)

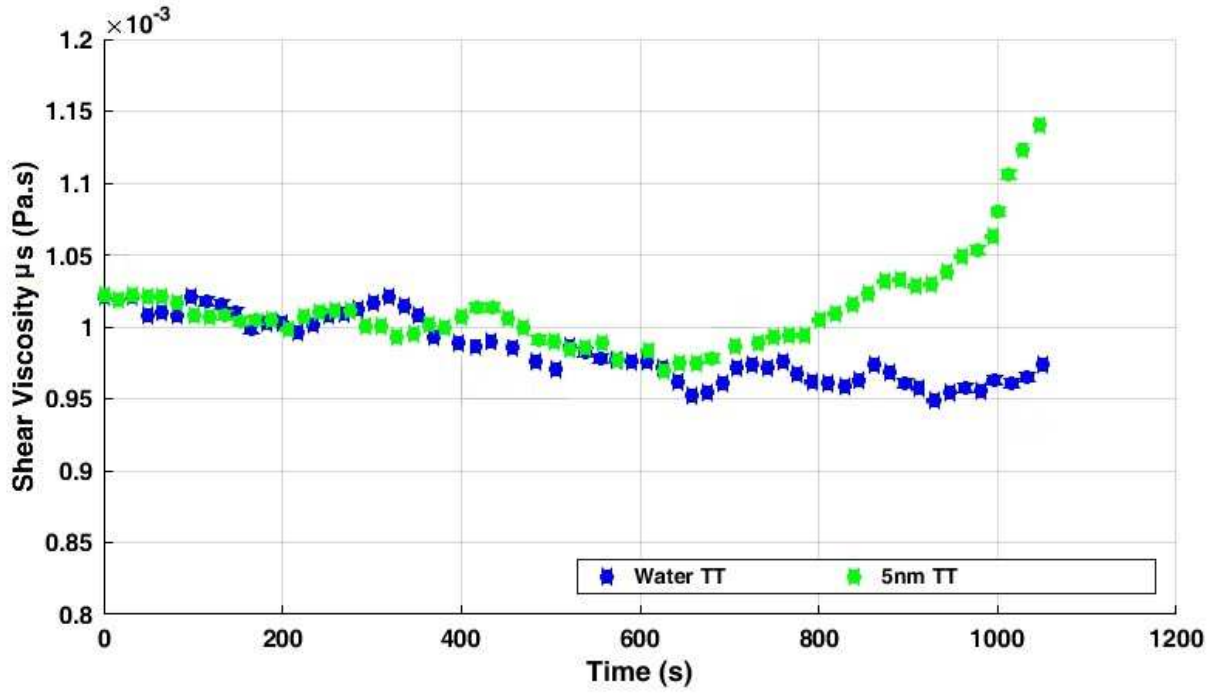
10



11

12 **Figure. 4.** Phase angle variation for water and Gold nanofluid droplet on a silicon substrate at  
13 22°C.

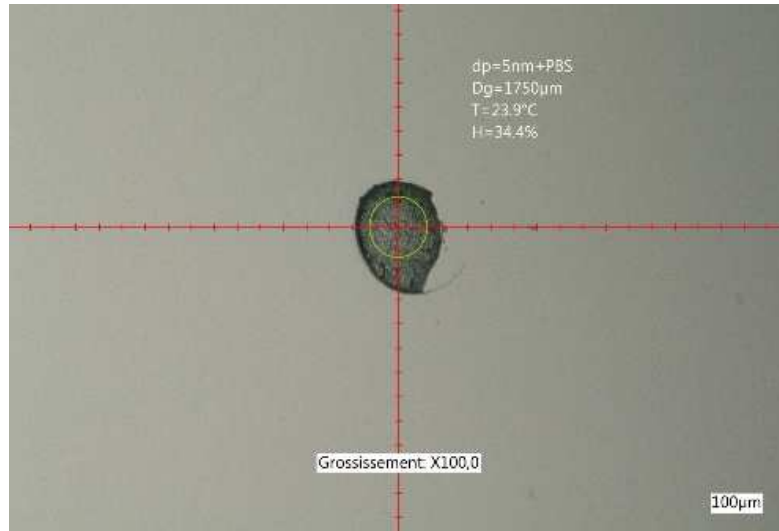
14



1  
2 **Figure. 5.** Shear viscosity variation during the evaporation of 4%  $C_v$  Au-water nanofluid droplet  
3 on a silicon substrate at 22°C.

4  
5  
6 **Fig. 5** presents the variation of dynamic shear viscosity of 4%  $C_v$  Au-water nanofluid sessile  
7 droplet during evaporation process at 22°C degree. The variation in the shear viscosity of gold  
8 nanofluids has the same value as water for the temperature 22°C [37], from the beginning till 800  
9 sec of the evaporation process (equal to  $0.97 \times 10^{-3}$  pa.s with  $\pm 0.002\%$ ). This behavior is due to  
10 the good stability of this type of gold nanoparticles were validation was proved in Zaaroura et al.  
11 [16]. After 800 sec, we noticed that the shear viscosity of gold nanofluid starts to increase while  
12 for water the values remains constant. The results obtained clearly showed the direct link  
13 between the deposits of gold nanoparticles on the shear viscosity of gold nanofluid. In the figure  
14 below, **Fig. 6**, we presented the final deposition of gold nanoparticles after the end of  
15 evaporation process where it observed clearly their deposition above the transducer which gave  
16 access to the concentration measurement later. (See section 3)

17



1  
2 **Figure. 6.** Gold nanoparticles final shape pattern on the 250 µm transducer diameter

3  
4 **3- Micromechanical model for nanofluids viscosity measurements**

5  
6 In order to validate our experimental results, a micromechanical model is presented to calculate  
7 the effective shear viscosity of nanofluids. This model is based on the Finite Element Method  
8 (FEM), using FreeFem++ software, which is compared to an analytical creep function that  
9 provides a way to extract the dynamic viscosity when a constant shear stress on the 2DKelvin-  
10 Voigt medium is applied, **Eq. (7)**. This new model based on the homogenization method has  
11 been validated and has proven its effectiveness for measuring the viscosity of different types of  
12 nanofluids, see the work of Zaaroura et al. [35].

13 Thus, it deals with complex situations such as nanofluids with a particle size distribution,  
14 concentration gradients, or particles of different materials.

$$\varepsilon = \varepsilon_{12} = \frac{\sigma_{12}^{\circ}}{2\mu} \left( 1 - e^{-\frac{\mu}{\mu_s} t} \right) \quad (7)$$

15  
16 Where  $\mu$  the lame constant,  $\varepsilon$  the deformation,  $\sigma$  the stress applied and  $\mu_s$  is the shear viscosity.

17 To apply this homogenization method, the concentrations of gold nanoparticles is needed. So,  
18 from the amplitude reflection coefficient of longitudinal waves  $R_{LL}$ , we were able to calculate the  
19 concentrations of gold nanoparticles deposited on the transducer during the evaporation process.

20 This correlation is represented in **Eq. (8)**

$$|R_{LL}| = \left| \frac{Z_{nf} - Z_{si}}{Z_{nf} + Z_{si}} \right| = \left| \frac{\rho_{nf} C_{nf}^L - Z_{si}}{\rho_{nf} C_{nf}^L + Z_{si}} \right| = \left| \frac{\sqrt{\rho_{nf} E_{nf}} - Z_{si}}{\sqrt{\rho_{nf} E_{nf}} + Z_{si}} \right|$$

$$\rho_{nf} = (1 - v_p)\rho_w + v_p\rho_p$$

$$E_{nf} = (1 - v_p)E_w + v_pE_p$$

(8)

$$\Rightarrow |R_{LL}| = \left| \frac{\sqrt{((1 - v_p)\rho_w + v_p\rho_p)((1 - v_p)E_w + v_pE_p)} - Z_{si}}{\sqrt{((1 - v_p)\rho_w + v_p\rho_p)((1 - v_p)E_w + v_pE_p)} + Z_{si}} \right|$$

1 Where  $\rho_{nf}$  and  $E_{nf}$  are the density and the young modulus of the nanofluid respectively,  $\rho_p$  and  
2  $E_p$  are the density and the young modulus of the gold nanoparticles and  $v_p$  is the particle volume  
3 fraction. In **Table 2**, we presented the volume concentrations of gold nanoparticles related to  
4 each amplitude reflection coefficient of longitudinal waves throughout the process of droplet  
5 evaporation. It is important to verify that the concentration of nanoparticles at the start of the  
6 evaporation process was found to be equal to zero and this because of the stability and the non-  
7 deposition of nanoparticles above the transducer. Whereas after the deposition has taken place,  
8 the increase in concentration is clearly observed until the end of the evaporation process.

9

10

11

Time (s)	0	200	400	800	1000	1030	1050
$ R_{LL}  \times 10^{-3}$	859.2	859.2	859.2	859.1	859	858.9	858.6
$C_v$ %	0	0	0	0.0128	0.015	0.017	0.021

12

13 **Table 2.** Gold nanoparticle concentrations deposited on the transducer during the evaporation  
14 process.

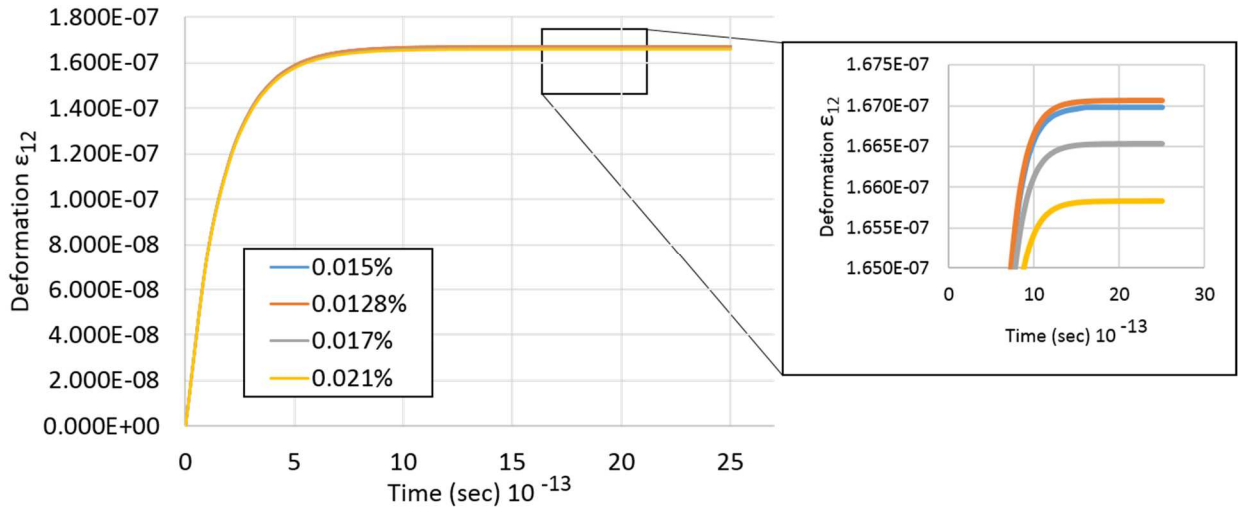
15

16 These concentrations were used to extract and calculate the viscosity of gold nanofluid from the  
17 homogenization model. The creep function is represented for each concentration after applying  
18 pure shear stress (**Fig. 7a**) and therefore calculate the dynamic viscosity using **Eq. (7)**. In **Fig.**  
19 **7b**, we have displayed the comparison between the acoustic experimental results and the  
20 theoretical results for the dynamic viscosity of gold nanofluid at different volume concentrations.



1 It the sensitivity and the precision of the differential variance of the creep function for these  
 2 concentrations were clearly demonstrated. Extracted results showed a very good agreement with  
 3 a relative error of around 6 %.

4

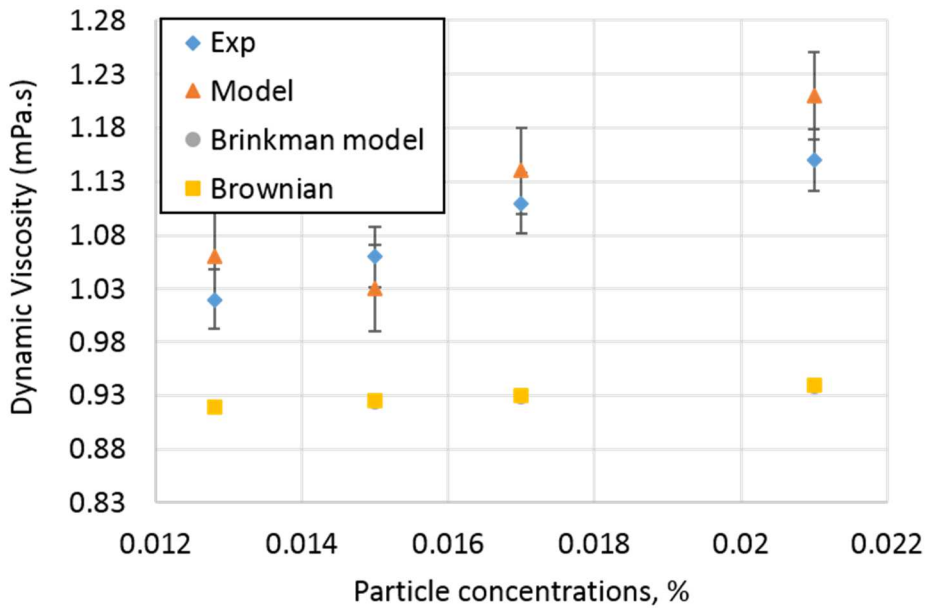


5

6

7

(a)



8

9

10

(b)

11 **Figure. 7.** (a) Shear creep function for the 2D-KV medium of Gold/water nanofluid at different  
 12 particle volume concentrations (i) 0.0128% (ii) 0.015% (iii) 0.017% (iv) 0.021%,

13 (b) Comparison of the dynamic viscosity of gold nanofluid with the acoustic experimental results  
 14 at ambient temperature.

15

1 For the same concentrations, we calculated the viscosity for each concentration using Brinkman  
2 and Brownian models. As the result showed, these viscosity prediction models are still not  
3 suitable due to their underestimation compared to experimental and real measurements.

#### 4 **IV- Conclusion**

5 An experimental study, based on a high frequency reflectometry principle (1-GHz), provided a  
6 detailed analysis to measure the dynamic viscosity of gold nanofluid at ambient temperature.  
7 This technique showed it's important to detect and investigate the interfaces (solid/liquid)  
8 depending on the reflection coefficients. The dynamic viscosity of gold nanofluid droplet (4%  
9 C<sub>v</sub>) was measured and followed during the evaporation process by measuring the mechanical  
10 impedance of the nanofluid droplet which has the complex form due to attenuation of the sound  
11 energy produced by it. The measurements **were** based on the longitudinal and shear reflected  
12 waves send from ZnO transducer to the interface. These two reflected waves enabled the  
13 extraction of the concentrations of gold nanoparticles deposited above the substrate from the  
14 longitudinal wave and to measure the dynamic viscosity based on these concentrations from the  
15 shear reflected wave.

16 On the other hand, a micromechanical model was used to validate the experimental results  
17 obtained by high-frequency acoustic waves. This model, based on a homogenization Kelvin-  
18 Voigt method, has validated its efficiency for nanofluids viscosity measurement applications.  
19 The results showed a very good agreement compared to the experimental data with a relative  
20 error of the order of 6%.

21

22

23

24

25

26

27

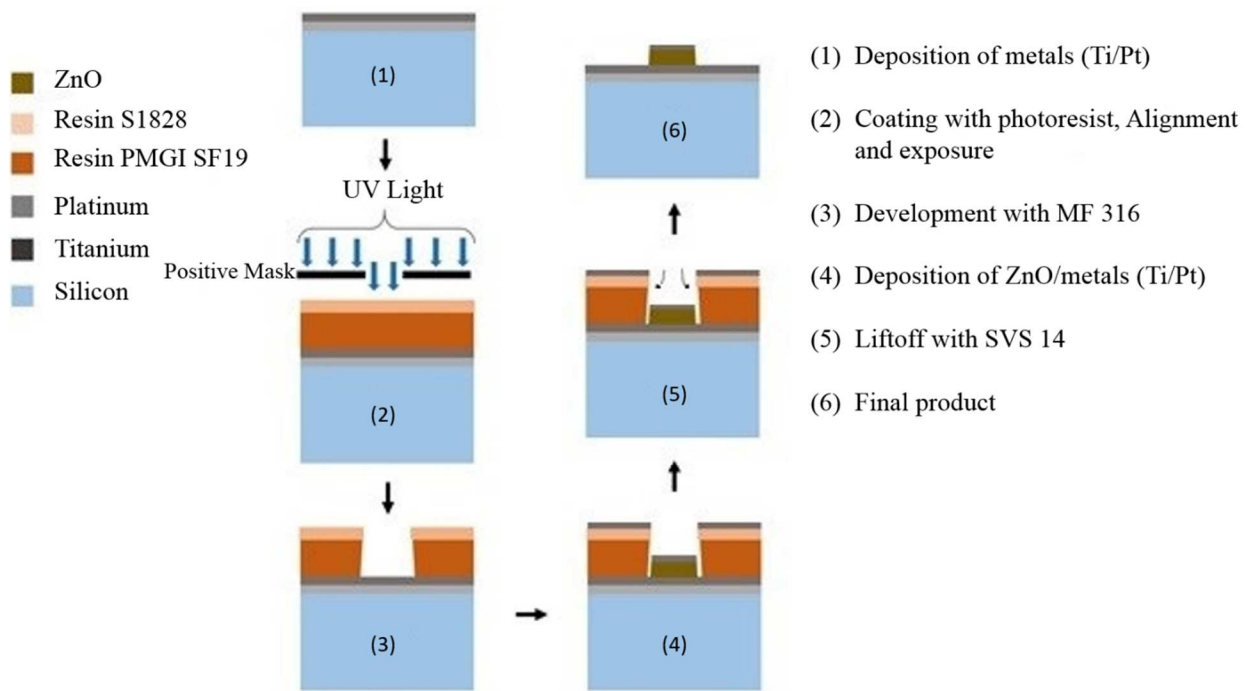
28

1 **Annex A**

2 ZnO transducer fabrication process:

3  
4 The fabrication of the used ZnO piezoelectric (1 GHz) is fabricated inside the clean room in Lille  
5 (France) and installed in the Institute of Electronic, Microelectronics and Nanotechnology  
6 (IEMN).

7 The fabrication procedure is shown below:



11 **Figure. 9.** Fabrication Process flow chart

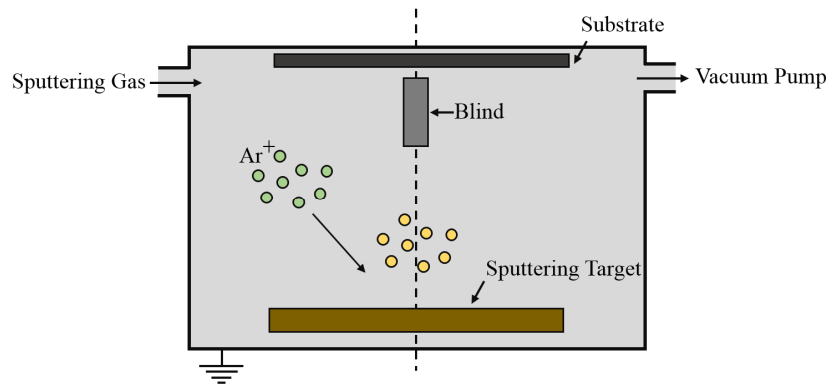
12 The fourth step, where the deposition ZnO is carried out, is performed using the Magnetron  
13 sputtering deposition frame, see **Fig. 10**, where the blind technique is applied, by placing an  
14 aluminum plate in the center of the substrate, inside the Magnetron chamber to generate more  
shear waves.



1

2

(a)



3

4

(b)

**Figure. 10.** (a) Magnetron sputtering system in real state (Institute of IEMN) (b) Magnetron sputtering system from inside with additional blind technique.

7

8

9

10

11

12

13

14

1 **Author Information**

2 Corresponding Authors

3 \*Email: Ibrahim.zaaroura@hotmail.com

4

5 **Acknowledgments**

6 The authors would like to acknowledge the financial support from Region ‘Hauts de France’, and  
7 CE2I-CPER for this work. We also want to thank the French Renatech Network for the support  
8 of the technological development.

9 **References**

- 10 [1] Sarit Kumar Das, Stephen U. S. Choi, Hrishikesh E. Patel, Heat Transfer in Nanofluids—A  
11 Review, Heat Transfer Engineering 27 (2006) 3-19, DOI: [10.1080/01457630600904593](https://doi.org/10.1080/01457630600904593)
- 12  
13 [2] J.M. Wu, J. Zhao, A review of nanofluid heat transfer and critical heat flux enhancement  
14 Research gap to engineering application, Progress in Nuclear Energy 66 (2013) 13-24.
- 15  
16 [3] Yu, W. and Choi, S.U.S, The role of interfacial layers in the enhanced thermal conductivity  
17 of nanofluids: A renovated Maxwell model, J Nanopart Res 5 (2003) 167-171.
- 18  
19 [4] M. Gupta, V. Singh, R. Kumar, Z. Said, A review on thermophysical properties of nanofluids  
20 and heat transfer applications, Renew. Sustain. Energy Rev. 74 (2017) 638-670.
- 21  
22 [5] I. Zaaroura, S. Harmand, J. Carlier, M. Toubal, A. Fasquelle, B. Nongaillard, Thermal  
23 performance of self-rewetting gold nanofluids: Application to two-phase heat transfer devices,  
24 Int. J. Heat Mass Transfer 174, (2021) 121322.
- 25  
26 [6] W.C. Wei, S.H. Tsai, S.Y. Yang, Kang, S.W. Kang, Effect of Nanofluid on Heat Pipe  
27 Thermal Performance, 3rd IASME/WSEAS Int Conf on Heat Transfer, Thermal Eng. Environ.  
28 (2005) 115-117.

29

- 1 [7] R. Sureshkumar, S. TharvesMohideen, N. Nethaji, Heat transfer characteristics of nanofluids  
2 in heat pipes: A review, *Renew. Sustain. Energy Rev.* 20 (2013) 397–410.
- 3
- 4 [8] L. Dongliang, P. Hao, L. Deqing, Thermal Conductivity Enhancement of Clathrate Hydrate  
5 with Nanoparticles, *Int. J. Heat Mass Transfer* 104 (2017) 566-573.
- 6 [9] W. XW, X. XF, C. SUS, Thermal conductivity of nanoparticle-fluid mixture, *Journal of*  
7 *thermophysics and heat transfer* 13 (1999) 474-480.
- 8 [10] Y. Zhu, M. Zamani, G. Xu, D. Toghraie, M. Hashemian, A. Alizadeh, A comprehensive  
9 experimental investigation of dynamic viscosity of MWCNT-WO<sub>3</sub>/water-ethylene glycol  
10 antifreeze hybrid nanofluid, *J. Mol. Liq.*, 333 (2021) 115986.
- 11 [11] A. Asadi, I.M. Alarifi, L.K. Foong, An experimental study on characterization, stability and  
12 dynamic viscosity of CuO-TiO<sub>2</sub>/water hybrid nanofluid, *J. Mol. Liq.*, 307 (2020), p. 112987.
- 13 [12] I. Zaaroura, M. Toubal, H. Reda, J. Carlier, S. Harmand, R. Boukherroub, A. Fasquelle, B.  
14 Nongaillard, Evaporation of nanofluid sessile drops: Infrared and acoustic methods to track the  
15 dynamic deposition of copper oxide nanoparticles, *Int. J. Heat Mass Transfer* 127, Part B (2018)  
16 1168-1177 <https://doi.org/10.1016/j.ijheatmasstransfer.2018.07.102>
- 17 [13] S.R. Yan, R. Kalbasi, Q. Nguyen, A. Karimipour, Rheological behavior of hybrid  
18 MWCNTs-TiO<sub>2</sub>/EG nanofluid: a comprehensive modeling and experimental study, *J. Mol. Liq.*,  
19 308 (2020), p. 113058.
- 20 [14] S. Umer Ilyas, R. Pendyala, M. Narahari, L. Susin, Stability, rheology and thermal analysis  
21 of functionalized alumina- thermal oil-based nanofluids for advanced cooling systems, *Energy*  
22 *Convers. Manage.* 142 (2017) 215-229; <https://doi.org/10.1016/j.enconman.2017.01.079>
- 23 [15] M.H. Esfe, H. Rostamian, M.R. Sarlak, A novel study on rheological behavior of ZnO-  
24 MWCNT/10w40 nanofluid for automotive engines, *J. Mol. Liq.*, 254 (2018), pp. 406-413.
- 25 [16] I. Zaaroura, S. Harmand, J. Carlier, M. Toubal, A. Fasquelle, B. Nongaillard, Experimental  
26 studies on evaporation kinetics of gold nanofluid droplets: Influence of nanoparticle sizes and  
27 coating on thermal performance, *Appl. Therm. Eng.*, 183 (2021) 116180.
- 28 [17] P. Chen, S. Harmand, S. Szunerits, R. Boukherroub, Evaporation behavior of PEGylated  
29 graphene oxide nanofluid droplets on heated substrate, *Int. J. Thermal Sciences*, 135 (2019) ,  
30 445-458.

- 1 [18] S.M.S. Murshed, K.C. Leong, C. Yang, Investigations of thermal conductivity and viscosity  
2 of nanofluids, Int. J. Thermal Sci. 47 (2008) 560-568;  
3 <https://doi.org/10.1016/j.jthermalsci.2007.05.004>
- 4 [19] Z. Jia-Fei, L. Zhong-Yang, N. Ming-Jiang, C. Ke-Fa, “Dependence of Nanofluid Viscosity  
5 on Particle Size and pH Value, Chinese Physics Letters, 26 (2009) no. 6, 066202.
- 6 [20] I. M. Mahbulul, R. Saidur, M. A. Amalina, Latest developments on the viscosity of  
7 nanofluids, Int. J. Heat Mass Transfer 55 (2012) 874-885;  
8 <https://doi.org/10.1016/j.jheatmasstransfer.2011.10.021>
- 9 [21] J.L. White, M.H. Han, N. Nakajima, R. Brzoskowski, The influence of materials of  
10 construction on biconical rotor and capillary measurements of shear viscosity of rubber and its  
11 compounds and considerations of slippage , J Rheol. 35, 167 (1991);  
12 <https://doi.org/10.1122/1.550226>
- 13 [22] T. Yiamsawas, A.S. Dalkilic, O. Mahian, S. Wongwises, Measurement and Correlation of  
14 the Viscosity of Water-Based Al<sub>2</sub>O<sub>3</sub> and TiO<sub>2</sub> Nanofluids in High Temperatures and  
15 Comparisons with Literature Reports, J. Dispersion Sci. Technol. (2013) 1697-1703  
16 <https://doi.org/10.1080/01932691.2013.764483>
- 17 [23] Brinkman HC. The viscosity of concentrated suspensions and solutions. J. Chem. Phys. 20  
18 (1952) 571-81.
- 19 [24] Einstein A. investigation on the theory of Brownian motion. New York: dover; (1956)
- 20 [25] Orozco. D, Hydrodynamic behavior of suspension of polarparticles. Encyclopedia surface  
21 colloid science 4 (2005) 2375-2396.
- 22 [26] P.N. Nwosu, J. Meyer, M. Sharifpur, Nanofluid Viscosity: A simple model selection  
23 algorithm and parametric evaluation, Comp Fluids 101 (2014) 241–249.
- 24 [27] A. Aminian, Predicting the effective viscosity of nanofluids for the augmentation of heat  
25 transfer in the process industries, J. Mol. Liq., 229 (2017) 300–308.
- 26
- 27 [28] S.A. Adio, M. Mehrabi, M. Sharifpur, J.P Meyer, Experimental investigation and model  
28 development for effective viscosity of MgO–ethylene glycol nanofluids by using dimensional

- 1 analysis, FCM-ANFIS and GA-PNN techniques, *Int. Commun. Heat Mass Transfer* 72 (2016)  
2 71-83.
- 3 [29] B. Mert, H. Sumali, O.H. Campanella, A new method to measure viscosity and intrinsic  
4 sound velocity of liquids using impedance tube principles at sonic frequencies, *Rev. Sci. Instrum.*  
5 75 (2004) 2613; [https://doi: 10.1063/1.1771489](https://doi.org/10.1063/1.1771489)
- 6 [30] H. Dahmani, I. Zaaroura, A. Salhab, P. Campistron, J. Carlier, M. Toubal, S. Harmand, V.  
7 Thomy, M. Neyens, B. Nongaillard, Fabrication and optimization of high frequency ZnO  
8 transducers for both longitudinal and shear emission: Application of viscosity measurement using  
9 ultrasound, *Adv. Sci. Technol. Eng. Syst. J.* 5(6), 1428-1435 (2020).
- 10 [31] W. P. Mason, W. O. Baker, H. J. Mckimin, and J. H. Heiss, Measurement of Shear  
11 Elasticity and Viscosity of Liquids at Ultrasonic Frequencies, *Phys. Rev.* 75 (1949) 936 – 1949.
- 12 [32] S. Chen et al., Shearwave dispersion ultrasound vibrometry (SDUV) for measuring tissue  
13 elasticity and viscosity, *IEEE Trans Ultrason, Ferroelectr Freq Control.* 56 (2009) 55-62.
- 14 [33] M.J. Holmes et al, Temperature dependence of bulk viscosity in water using acoustic  
15 spectroscopy, *J. Phys. Conf. Ser.* 269 (2011) 012011; [https://doi.org/10.1088/1742-](https://doi.org/10.1088/1742-6596/269/1/012011)  
16 [6596/269/1/012011](https://doi.org/10.1088/1742-6596/269/1/012011)
- 17 [34] S. Li, J. Carlier, M. Toubal, H. Liu, P. Campistron, D. Callens, G. Nassar, B. Nongaillard, S.  
18 Guo, High frequency acoustic on-chip integration for particle characterization and manipulation  
19 in microfluidics, *Appl. Phys. Lett.* 111 (2017) 163503.
- 20 [35] Zaaroura, I., Reda, H., Lefebvre, F. et al. Modeling and Prediction of the Dynamic Viscosity  
21 of Nanofluids by a Homogenization Method. *Braz J Phys* (2021). [https://doi.org/10.1007/s13538-](https://doi.org/10.1007/s13538-021-00909-4)  
22 [021-00909-4](https://doi.org/10.1007/s13538-021-00909-4).
- 23 [36] S.P. Nikanorov, Y.A. Burenkov, A.V. Stepanov, Elastic properties of silicon, *Sov. Phys.*  
24 *Solid State.* 13 (1972) 2516–2518.
- 25 [37] L. Korson, W. Drost-Hansen, F. J. Millero, Viscosity of water at various temperatures, *J.*  
26 *Phys. Chem.* 73 (1969) 34-39; [DOI: 10.1021/j100721a006](https://doi.org/10.1021/j100721a006)

27